C(S)

Numerical Simulation of Environmental Modulation of Chemical Signal Structure and Odor Dispersal in the Open Ocean

Ronald C. Baird, Hamid Johari[1] and George Y. Jumper[2]

Departments of Biology and Biotechnology and [1]Mechanical Engineering, Worcester Polytechnic Institute, 100 Institute Road, Worcester, MA 01609 and [2]Aerospace Engineering Division, US Air Force Phillips Laboratory, Hanscom AFB, MA 01731, USA

Correspondence to be sent to: R.C. Baird, Director, National Sea Grant College Program, 1315 East-West Highway, Room 11716, Silver Spring, MD 20910, USA

Abstract

Hydrodynamic models were used to simulate the dispersal of a model fish pheromone at three characteristic depth regimes (mixed layer, and 300 and 1000 m) of broad extent in the open ocean at the scale of individual organisms. The models were calibrated to experimental studies of dye dispersal at these depths and the goldfish pheromone system was used as the model odorant. There are profound differences in the time course and geometry of dispersing odor fields with depth. Below the thermocline odor fields spread primarily as horizontal patches with dispersal rates about five times slower at 1000 m as compared to 300 m. In the mixed layer, odors disperse rapidly in all directions and the maximum radial distance of spread of a physiologically active odor patch is less than half of the deep water value. Increases in the threshold sensitivity of olfactory receptors can greatly increase effective odor field size. Chemical signals impact the encounter dynamics among oceanic organisms by affecting the distance at which the target (emitting) individual is perceived. Perception distances due to olfactory cues can be significantly greater than for other senses in pelagic oceanic environments. Environment specific modulation of odor fields then affects the signal properties and therefore utility of chemoreception that, in turn, bear on encounter probabilities and transfer functions in oceanic ecosystems. **Chem. Senses 21: 121–134, 1996.**

Introduction

Knowledge of the dynamics of space, time and scale in the distribution of organisms is essential to a better understanding of the processes structuring natural communities in the sea (Levin, 1990; Angel, 1994) and the properties of the physical environment are increasingly recognized as critical to that understanding (Roughgarden *et al.*, 1988; Giller *et al.*, 1994). Chemical signals are subject to significant modulation by the physical environment (e.g. Moore *et al.*, 1994) and chemoreception is known to be important to many ecological processes in aquatic environments that bear on the reproduction, distribution and abundance of resident animal populations (Hara, 1986; Sorenson and Stacey, 1990). Olfactory organs are well developed in a broad spectrum of oceanic organisms (Marshall, 1967; Derby and Atema, 1988; Finger, 1988; Baird *et al.*, 1990) indicative of the importance of odor cues in the sea. A critical step in better understanding the role of chemoreception in the ecosystem dynamics of the ocean is greater knowledge of the environmental

modulation of odor cues as a product of the physical environment.

Recently, much progress has been made in understanding the transport of chemical signals in aquatic environments (Moore and Atema, 1991; Westerberg, 1991; Weissburg and Zimmer-Faust, 1993; Moore *et al.*, 1994). These studies have been directed primarily at understanding odor signal structure at small scales in moving waters with varying substrate characteristics. The open ocean is less well studied at small scales though several investigations provide data suitable for developing a theoretical basis for small scale dispersion of chemical substances in the open ocean (Schuert, 1970; Ewart and Bendiner, 1981; Atema, *et al.*, 1991). More recently, Jumper and Baird (1991) have studied the problem of chemical signal transport as it relates to the reproductive biology of deep-sea fishes at mid-depths of the ocean.

Here, we extend the work of Jumper and Baird (1991) in investigating the dynamics of odor dispersal in the sea. We chose, for numerical analysis, three characteristic depth horizons representative of open ocean environments of broad geographic extent. Hydrodynamic models are used to depict the geometry and time course of dispersal of model odor fields in these oceanic environments at the scale of individual organisms. The numerical models have been calibrated to actual oceanic conditions. Characteristics of known fish pheromone systems are used to provide the appropriate scale for the numerical simulations. The results of the analysis are then discussed from the perspective of odor signal transmission and source location for organisms inhabiting the modeled environments.

Numerical simulation

Environmental setting

The vast majority of the surface area of the world's ocean is characterized by a stable water column throughout much of the upper 2000 m or more in depth. This is particularly true in the large central gyre regions of subtropical seas where the data sets used to calibrate the numerical models used here were derived (Schuert, 1970; Ewart and Bendiner, 1981; Gregg, 1987). These oceanic areas exhibit a typical vertical structure in which there is a relatively well mixed surface layer of about 20–150 m in depth followed by a sharp temperature and density gradient extending to about 1000 m followed by a much less marked density gradient below that depth (Ross, 1988; Kennish, 1994). These characteristic physical features strongly affect the manner in which turbulent diffusion acts on odor fields as a function of depth.

In addition to their characteristic year round stability and vertical structure, large, subtropical open ocean environments exhibit little detectable current structure in the upper 1000 m at the scales of interest here. Strong currents may be detectable near bottom (Atema *et al.*, 1991) and at large scales (Schuert, 1970) in the ocean. However, at scales of 500 m and less the distortion effects of current vectors were undetectable 46 h after dye release in two separate experiments (Schuert, 1970; Ewart and Bendiner, 1981). In one case, the dye field moved over 12 km under prevalent currents, yet the patch was not severely distorted (Schuert, 1970). The importance for our purposes is that, at the scales of interest, chemical substances in these environments disperse symmetrically in the horizontal rather than along a specific directional vector as would be the case, for instance, in a flowing stream.

For purposes of numerical simulation then, we chose to model dispersion at three depths representative of diffusion environments characteristic of central water masses in the world's oceans. These depths were also chosen because data sets are available from which to calibrate the hydrodynamic models used. A near-surface depth horizon of about 20 m was chosen to represent turbulent, mixed layer environments. Two depths were chosen as representative of highly stratified conditions found below the permanent thermocline. The two depths chosen (300 and 1000 m) also exhibit very different thermal and light regimes for resident organisms.

While hydrodynamic models allow one to simulate the dispersion of chemical substances in the ocean, values for the basic parameters of interest are unspecified. To provide a spatial scale relevant to individual organisms, we chose values derived from studies of goldfish pheromones. The goldfish system has been documented in detail by Sorenson and his colleagues (Sorensen and Stacey, 1990; Sorenson, 1992) and is among the best known fish chemosensory system. The above authors report that female goldfish release approximately 77 ng/h of a water soluble, pre-ovulatory hormone that is highly stimulatory in males. Furthermore, they report that males have a detection threshold for the pheromone of approximately 10^{-13} M. The pheromone may degrade with time. For purpose of simulation then, we assumed that all 77 ng of pheromone are released at a single instant in time, that the detection threshold is 10^{-13} M and the first order decay term k is set to a half life of 6 h to simulate loss of activity with time.

The intention here is not to explicitly mimic the goldfish system, but rather to scale a model system that has features in common with those found in a known natural system.

The model can then be used to explore the general characteristics of chemical signal dispersal in the habitats of interest.

Hydrodynamic diffusion models

Diffusion of miscible matter in a fluid at rest occurs by molecular motions, i.e. Fickian diffusion, and it is characterized by the diffusion coefficient D. For a constant diffusion coefficient, the equation for the concentration field $C(x,t)$ is

$$\frac{\partial C}{\partial t} = D\nabla^2 C \tag{1}$$

In an infinite domain, the solution of the above equation subject to an instantaneous point source at the origin is a gaussian expression as follows:

$$C(r,t) = \frac{M}{(2\pi\sigma^2)^{3/2}} \exp\left(-\frac{r^2}{2\sigma^2}\right), \tag{2}$$

where M is the source mass, r and t represent the radial distance from the source and time, respectively. The variance σ^2 is equal to $(2Dt)$.

If the fluid is in motion, two new phenomena appear, namely advection and diffusion due to mechanical stirring. The latter is termed 'turbulent diffusion' when the flow is in turbulent state, the most likely case in oceanic scenarios. It has been shown that the above expressions are not valid in the presence of oceanic turbulent flows (Murthy, 1976; Okubo, 1971). The generalized equation of turbulent diffusion for the mean concentration $\overline{C}$ is

$$\frac{\partial \overline{C}}{\partial t} + (\vec{u}\cdot\nabla)\overline{C} = D\nabla^2\overline{C} + \nabla\cdot\vec{J} - k\overline{C}, \tag{3}$$

where $\vec{u}$ is the mean velocity vector field and

$$\vec{J} = \left(E_x\frac{\partial \overline{C}}{\partial x}, E_y\frac{\partial \overline{C}}{\partial y}, E_z\frac{\partial \overline{C}}{\partial z}\right)$$

the flux vector consisting of the apparent turbulent (eddy) diffusivity E multiplied by the concentration gradient in the three Cartesian directions. Therefore, knowledge of both the mean flow field, as well as the apparent diffusivities, which depend on the flow field small scale details, are needed to determine the mean concentration field. Unfortunately, neither the apparent diffusivities nor the mean flow field are readily available in a given oceanic volume at any time since these parameters depend greatly on the local/global conditions. It is noteworthy that in the majority of turbulent flows, the middle term $(\nabla\cdot\vec{J})$ on the right hand side of equation 3 is several orders of magnitude greater than the molecular diffusion term $D\nabla^2C$ and, therefore, the latter is ignored. In other words, molecular diffusion is negligible in comparison with turbulent diffusion.

An alternative approach to solving the turbulent diffusion equation for a patch of miscible matter is to assume that the dispersion can be broken into two separate identifiable parts, the advection of the entire patch by the mean flow field, and turbulent diffusion with respect to the 'center of patch' (Csanady, 1973). Then, the turbulent diffusion equation reduces to

$$\frac{\partial c}{\partial t} = \nabla\cdot\vec{J} - kc, \tag{4}$$

where c denotes concentration field in a co-ordinate system moving with the 'center of patch'. Except for the decay term, the above equation is very similar to equation 1 and, in fact, the two become identical if the apparent diffusivities are set equal to the molecular diffusion coefficient.

In the majority of flows, the general solution to equation 4 turns out to be a gaussian once a number of instantaneous individual profiles are averaged. An example of this is provided by Csanady (1966) where a number of concentration profiles were measured across a continuous dye plume released into Lake Huron. Although each individual profile is different from a gaussian distribution due to the eddy distortions in the turbulent surface layer of the lake, an average of only 25 profiles provided a very nearly gaussian concentration distribution. Furthermore, the peak concentrations measured in a number of instantaneous profiles appear to be within ±50% of the mean (peak) value of the gaussian distribution. In other words, modeling an instantaneous concentration profile by a gaussian, although strictly inaccurate, can be a viable approach as long as the reference frame advects with the flow field. Moreover, no other alternatives to statistical averages exist for modeling diffusion in turbulent flow fields.

To proceed further, we will assume a gaussian solution for equation 4 as follows:

$$c = \frac{M}{(2\pi)^{3/2}\sigma_x\sigma_y\sigma_z}\exp\left[-\tfrac{1}{2}\left(\frac{x^2}{\sigma_x^2}+\frac{y^2}{\sigma_y^2}+\frac{z^2}{\sigma_z^2}\right)-kt\right]. \tag{5}$$

Since flow properties vary greatly with depth in the ocean, different models for variances were chosen, each according to the physical environment in the water column. A hydrodynamic model was developed first for a near surface or

mixed layer habitat usually defined as a depth horizon occurring from near the surface to the beginning of the thermocline that is generally found at a depth of 20–150 m in mid to low latitudes of the world's oceans (Kennish, 1994). Here, turbulence disperses chemical signals in all directions and Csanady (1973) provides the variances for a dye patch in homogeneous turbulence at various growth stages. A brief description of these growth stages is presented below.

When the patch is much smaller than the smallest turbulent length scales, patch growth proceeds by molecular diffusion processes. The smallest turbulent scales in the ocean are approximately a few millimeters (Caldwell, 1983). The expected pheromone patch at the release instant can be argued to be of the same dimensions and, therefore, this initial growth phase is not applicable here. The next growth phase assumes isotropic conditions which implies that the three variances are all equal. Theory of homogeneous turbulence (Batchelor, 1950) provides the appropriate expression for the variance as a function of the dissipation rate of turbulence ε (i.e. energy dissipated by turbulence per unit time for a unit mass) as follows.

$$\sigma_x^2 = \sigma_y^2 = \sigma_z^2 = 2(a\varepsilon t^2)t \tag{6}$$

In the above expression a is a proportionality constant of order unity. Notice that the variances, which are related to the patch dimension, grow quite rapidly with time (as t^3). Okubo (1971) has assembled a large number of data sets from diffusion in various oceanic conditions and has shown that the above expression agrees with experimental measurements. Replacing for variances in equation 5 results in an expression for the mean concentration field in homogeneous turbulence,

$$c(r,t) = \frac{M}{8(\pi\varepsilon t^3)^{3/2}} \exp\left[-\frac{r^2}{4\varepsilon t^3} - kt\right], \tag{7}$$

where r is the distance from the 'center of patch' in the moving reference system and k represents the decay term. When M is in terms of moles released and ε has units of W/kg, the concentration c will have units of mol/m^3. An average value for the dissipation rate of turbulence ε in the ocean at depths of 20–60 m is 10^{-7} W/kg (Gregg, 1987). The actual value of ε depends on geographic location, seasonal temperatures and storms, etc.

The expression in equation 7 is valid until the patch grows to a size comparable to the large eddies of turbulence, beyond which the growth rate slows down. As it turns out, the pheromone patches of interest, with length scales of less than 100 m, do not grow to the extent of the large turbulent eddies (in the order of kilometers) in the mixed layer. Therefore, the last stages of growth will not be discussed here. It suffices to state that for pheromone patch diffusion in the mixed layer, the expression in equation 7 provides the concentration in a reference frame moving with the 'center of patch'.

Below the thermocline the geometry of dispersal of chemical substances is markedly different from the surface. The highly stratified nature of the water column in these midwater habitats results in little vertical diffusion in comparison with rates of horizontal diffusivity, i.e. $\sigma_z << \sigma_x, \sigma_y$. The resulting patch geometry is best described by a horizontal area of nearly uniform thickness (Schuert, 1970). In order to model the diffusion in the midwater regions of the ocean, we have adapted an expression for horizontal variances first developed by Joseph and Sendner (1958). Assuming equal values for the two horizontal variances, $\sigma_x = \sigma_y$, the expression is:

$$\sigma_x\sigma_y = 3P^2t^2, \tag{8}$$

where P is the parameter describing the diffusion processes and is referred to as 'diffusion velocity' (m/s). The horizontal variances here grow less rapidly (t^2) as compared to the ones near the surface (t^3).

To complete the formulation for this region of ocean, we also need to characterize the vertical variance σ_z. Although several estimates have been provided for this parameter, it appears that a constant vertical patch thickness is the simplest form and has been observed in oceanic dye dispersion experiments. Combining the horizontal diffusivities of equation 8 and a constant vertical patch thickness results in a concentration field, with respect to the 'center of patch', for the region below the thermocline as follows.

$$c(r,t) = \frac{M/h}{2\pi(Pt)^2} \exp\left[-\frac{r}{Pt} - kt\right] \tag{9}$$

where h is the vertical thickness of the odor patch. In the above equation, r denotes the radial distance in the horizontal plane from the 'center of patch'. Equation 9 was found by Schuert (1970), and Ewart and Bendiner (1981) to describe well the diffusion of chemical dyes at two widely separated subtropical environments where these investigators determined by experiment that values of P of about 1.3×10^{-3} m/s (300 m) and 2.7×10^{-4} m/s (1000 m) best fit their data. These values were used in Equation 9 to depict odor dispersal in upper (300 m) and lower (1000 m) mesopelagic habitats, respectively. It should be noted that in Schuert's

(1970) study the patch thickness (h) did not significantly increase at a depth of 300 m over 48 h during which time mass transport moved the dye patch several kilometers from the release point. Moreover, Ewart and Bendiner (1981) found 'little evidence of severe distortion of the patch by eddy activity' at horizontal patch scales of 200 m or less.

To estimate patch thickness (h) we assumed that initially the patch grows rapidly in the wake of the emitting organism and then is stabilized due to stratification. Assuming wake velocities on the order of one mm/s and buoyancy frequency of 0.01 s^{-1} results in a length scale on the order of 10 cm which appears consistent with other studies of buoyancy length ranges in highly stratified waters (Denman, 1994).

It has to be emphasized that the expressions in equations 7 and 9 are idealistic models of the actual turbulent concentration field for any given instantaneous release in a frame of reference moving with the 'center of patch'. The parameters P and ε vary with local/global conditions, and the values chosen are only to provide a comparison of diffusion processes in different settings. In the stratified regions, effects of eddy distortions are negligible while near the surface there is perhaps appreciable distortion of the patch. The intent here to provide reasonable estimates and limits rather than exact quantitative values.

Simulation results

Equations 7 and 9 were solved for r given the threshold value (C^*) for the goldfish pheromone (i.e. 10^{-10} moles m^{-3}), and parameters ε and P were set at values described above. Pheromone (77 ng) was released at a single instant in time and prior to release the background concentration was everywhere zero. The results of the numerical simulations for the three environments appear in Figure 1.

The results depict reasonably well the idealized time course of dispersal in the three habitats particularly prior to the maximum extent of the odor field. The results shown in Figure 1 illustrate the profound differences in the modulation of odor dispersal in each of the three habitats. In addition to the three- versus two-dimensional dispersal characteristics of the mixed layer and mid-water habitats, respectively, there are major differences in both the extent and time course of spread of the 'active' pheromone patch. Near the surface, the pheromone signal has a limited, maximum range (albeit in three dimensions) and is rapidly dispersed by turbulence. The whole sequence occurs in several minutes in this example.

At mid-depths the narrow odor patches have greater horizontal extent and take much longer to disperse. At 1000 m the diffusion velocity P is almost five times less than at 300 m.

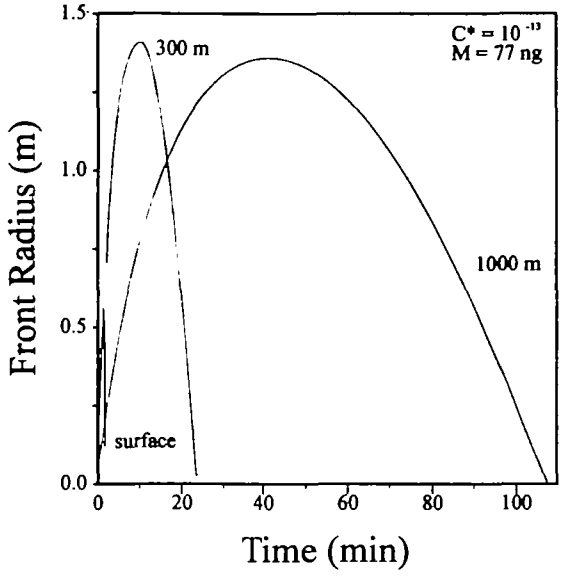

Figure 1 Time evolution of the front of an active patch in three different oceanic settings (see text). The spherical signal in the mixed layer appears spikelike in comparison to odor fields at 300 and 1000 m depths

It should be noted that the goldfish pheromone system in these simulations is effective only in the near field in all three habitats. Ranges are limited to less than 1.5 m from the emitting individual. At 1000 m, however, the signal takes well over an hour to fully dissipate. In the ocean, such a system would have limited utility for long range communication, perhaps not surprising given the freshwater environments inhabited by this species.

Since the concentration gradients in a pheromone field are important in source location (Jumper and Baird, 1991), we examined the gradient structure as a function of time and (horizontal) radial distance from the emitting source. Figure 2 depicts the radial distribution of the pheromone patch at 300 m at 3, 9 and 18 min after the release. Although the concentration gradients are very sharp at small times after release, they decline as time progresses. The 9-min mark approximately corresponds to the concentration profile near the maximum extent of the active patch (Figure 2). The two other times are included for comparison of the concentration gradients before and after the patch has reached its maximum radial extent. Under single emission conditions, odor fields should be most effective for source location prior to the maximum extent of the active patch when gradients

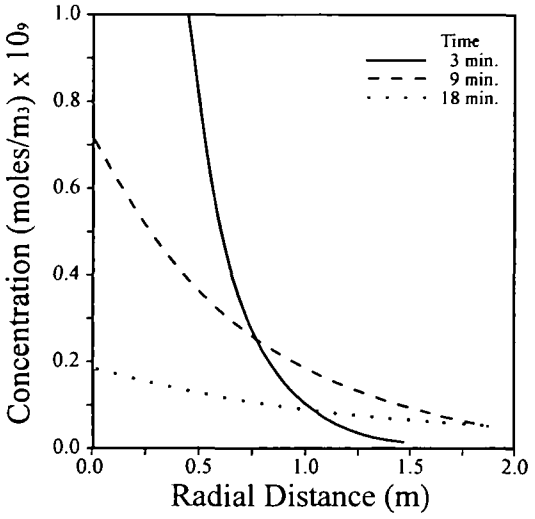

Figure 2 Mean concentration profiles at 3, 9 and 18 min after an instantaneous release at 300 m. The 9-minute mark approximately corresponds to the maximum extent of the active patch. The baseline threshold concentration is 10^{-10} mol/m^3.

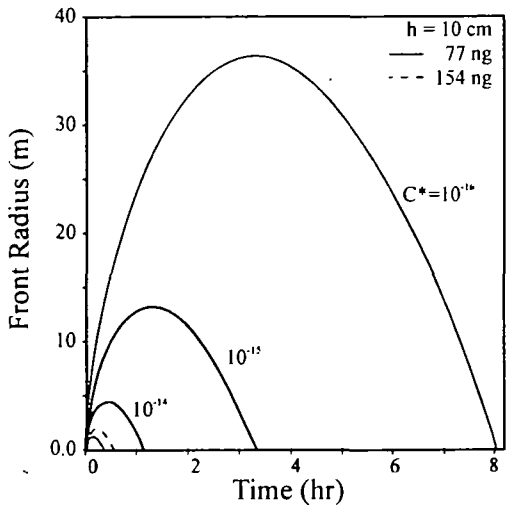

Figure 3 Time evolution of active patch fronts after instantaneous odorant release at 300 m as a function of increasing olfactory sensitivity. The baseline threshold concentration (10^{-13} M) curves are unlabelled. The dashed line represents a doubling of odorant mass released for the baseline case.

are most pronounced and potential patch distortions due to turbulence less marked.

The dramatic effects of increasing olfactory sensitivity by up to three orders of magnitude are depicted in Figure 3 for the 300 m case. Such sensitivities have been reported in vertebrates (Moulton and Marshall, 1976). Increasing sensitivity produces longer residence times and logarithmic increases in size of the active patch. Increases in pheromone mass (M) have a similar effect on patch size and Figure 3 depicts a doubling of pheromone mass released while holding sensitivity constant. Molecular decay has a relatively small effect prior to the patch reaching its maximum radius, but could be important later in the dispersal phase (Jumper and Baird, 1991).

Discussion

Physical models

The models are used here to explore chemical dispersion at the scale of individual organisms ranging in size from about one to 50 cm in length. Odor sources from such organisms might produce active odor patches that range from centimeters to 100 m or more at maximum diameter. At these scales, dispersion of odors is determined by 'effective' diffusivity resulting from turbulent mixing, the collective sum of small scale water motions at the depth of interest. These small turbulent events are encompassed in the ϵ term of the homogeneous turbulence model and the P term in the Joseph and Sendner (1958) expression. These rates of dispersion exhibit surprisingly modest variance over large geographic distances (Gregg, 1987). For instance, Schuert (1970) determined the value of P (300 m) to be 1.3×10^{-3} m/s in the Kauai Channel off Hawaii where a significant current moved the dye field some 12 km to the north-east after release. Ewart and Bendiner (1981), using different methods, determined P (300 m) at a location about 600 miles off San Diego to be 1.0×10^{-3} m/s.

These studies considered scales of from about 10 m to almost 2 km (Figure 4). Thus, while we are less certain of the accuracy of these models for prediction at scales of a couple of meters or less, they appear to predict reasonably well the dispersion characteristics of chemical substances over much of the ocean at the depths of interest at scales of less than 200 m.

It should be kept in mind that the models provide the essential effects of turbulent mixing due to the flow field while ignoring the movement of the patch. This is a Lagrangian point of view as opposed to an Eulerian one in which the reference frame is held stationary. The advantage is that the details of the flow field needed for the bulk movement of the patch are not required. Moreover, the models are valid exclusively for developed turbulence (at high Reynolds/Peclet numbers) and molecular diffusion has been ignored.

Concerning advection, while large scale currents and

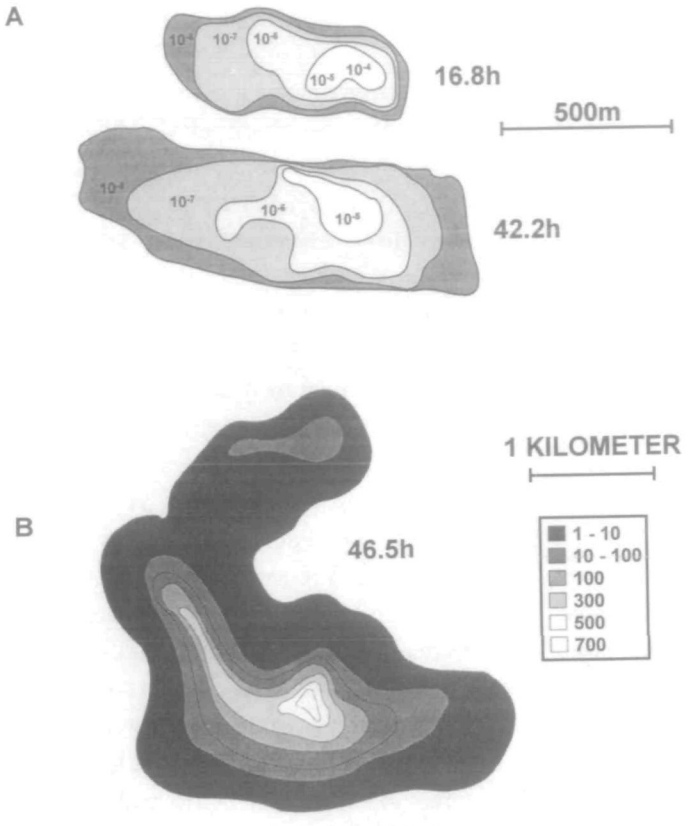

Figure 4. Two-dimensional plots of dye concentration (g/cm^2) fields: **(A)** is at a depth of 1000 m, 16.8 and 42.2 h after initial dye release, about 600 miles south-west of San Diego (adapted from Ewart and Bendiner, 1981) and **(B)** is at a depth of 300 m 46 5 h after dye release in the Kauai channel off the island of Oahu, Hawaii (adapted from Schuert, 1970). Scale in (B) is $\times 10^{-8}$ g/cm^2

eddies, particularly along shear fronts, are well known in the open ocean (Holland and Rhines, 1980; Pickart, 1988), the scales of interest are generally much larger than considered here (i.e. 10–500 km). At those scales, mass flow moves organisms and associated odor patches at equal velocities such that directional advection is not apparent in a diffusing odor patch. Convincing evidence is provided by Schuert (1970) where, after having been moved by large scale currents some 12 km from point of release, he was able to calculate reasonable mass balances from the symmetrically dispersing dye patch some 46.5 h after release (Figure 4). For that reason no directional advection terms were included in our models.

These assumptions clearly break down in the vicinity of fixed substrates which provide both opportunities for organisms to orientate to local currents, and for local substrate-induced turbulence to introduce both convective and advective forces to odor patches. Recent studies, for instance, have shown the very patchy and non-symmetrical structure of odor signals due to current induced turbulence in the deep ocean (*c.* 900 m) near the bottom (Atema *et al.*, 1991).

Although more recent models for dispersal and advection in the near shore regions of the ocean have been developed (Parslow and Gabric, 1989), these models only provide a means for estimating a patch size rather than the actual concentrations within the patch. These models are applicable to larger (time and space) scales, typically days and kilometres. Furthermore, the basis of these models is the notion that the patch variance increases with time cubed, consistent with our expression in equation 6.

Finally, it is important to consider the role of turbulence in both distorting the geometry of odor patches from the idealized shapes depicted in our models and, more importantly, in creating heterogeneity at the very small temporal and spatial scales sampled by chemosensory organs in aquatic organisms. In the upper or surface mixed layer, turbulence can vary by several orders of magnitude from the wind-mixed upper few meters to more stable conditions at depths of 20 m or more. Furthermore, conditions can vary particularly under high wind or storm conditions. Very near the surface odor fields encounter the air/surface interface and tend to disperse primarily in two dimensions (Okubo, 1980). For odor patches in nature in the mixed layer, one can expect rapid distortion from an idealized spherical geometry with time and distance from an odor source. This results in both rapid dispersion of odors and patchy signal strength at very small time and space scales.

In the highly stratified waters below the thermocline, effective turbulence is greatly reduced from mixed layer values and appears to continue to decrease with depth at least to 1000 m (Ewart and Bendiner, 1981). Furthermore, there appears to be little vertical spreading of the signal though further research is required to better understand the size structure of microdensity gradients in the sea and their effect on odor patch geometry at the scales of interest here. The critical points of biological significance are that these deep water odor fields are highly stable for long periods of time, that dispersion is primarily in the horizontal direction and that marked concentration gradients are maintained for significant periods of time.

Figure 4(a) shows two horizontally spreading dye patches at 1000 m (adapted from Ewart and Bendiner, 1981) at 16.8 and 42.2 h after initial dye release, 600 miles south-west of San Diego. Note the high coherence of the patches, the modest distortion from the idealized geometry and the

symmetry of dispersion at a scale of 500 m. Figure 4(b) shows a dye patch at 46.5 h (adapted from Schuert, 1970) at 300 m in the Kauai channel off the island of Oahu. The scale in this plot is 1 km and all the contours are the measured, vertically-integrated dye concentration (g/cm^2) field. Gray scale shading is used to emphasize the existence of sharp concentration gradients as well as the relatively modest distortions after long periods. It should be kept in mind that the diffusion parameter P is five times smaller at 1000 m than at 300 m. In encountering these patches, the above investigators note that there is always an abrupt signal change at the patch vertical margin, that shapes are symmetrical, log concentration gradients can be as close as a few meters, and at scales of 200 m or less there is little evidence of distortion of the patch by eddy activity.

Biological implications

The ubiquity of chemoreceptor organs found in oceanic nekton attests to the importance of odor cues in these environments. Rittschof (1992) lists some 10 chemically-mediated behavior patterns known in crustaceans, among the more important being reproduction and feeding. These behavior patterns are known to be chemically mediated in fishes as well (e.g. Kleerekoper, 1969, 1978; Atema *et al.*, 1980; Sorenson, 1992). Marshall (1967) remarks that in about 80% of the pelagic deep-sea fishes he investigated, large, well developed olfactory organs were found in males. Baird *et al.* (1990) found well developed olfactory organs in both sexes in two species of mesopelagic fishes, in addition to sexual dimorphism. This argues strongly for both the presence and importance of pheromones in the deep-sea.

We have chosen to model a single release case based on the known hourly production of a goldfish pheromone. Little is known about actual release rates in goldfish, only the integrated amount released over 1 h. In nature, goldfish release pheromone over an extended period of up to 7 h with rates peaking over several hours (Sorensen and Stacey, 1990). Urine in salmonids is released at about 30-min intervals (Curtis and Wood, 1991) and if in goldfish (and other small pelagic fishes) pheromones are released in the urine in similar fashion, then multiple releases of pheromones may be common. At present, we know nothing about pheromone release rates (or the pheromones themselves) in pelagic open ocean fishes or invertebrates.

Depending on the frequency of release and movement of emitting organisms, complex, time dependent and fluctuating geometries in odor patches can result. Jumper and Baird (1991) modeled the special case of a continuous release with the emitting organism remaining stationary. In this case the active patch reaches an equilibrium and mean signal strength does not decay over time at a given distance from the source. The basic physics of dispersal for multiple release cases are the same as for single releases. There is evidence that fluctuations in signal strength are effective in eliciting responses from chemoreceptors, at least in invertebrates (Gomez *et al.*, 1994).

Likewise, we know little about the loss of activity of pheromones or other biologically active odors. Organic substances in the sea are subject to bacterial and chemical degradation. Decay can be expected to affect most organic odor causing substances. Our model includes decay simply to examine its consequences. Unless decay is rapid, the effects are negligible at the temporal scales used here. Only when organisms are sufficiently dense and emitting frequently (or continuously) would we expect background concentrations of a chemical signal to be relevant.

Odorant release mass can be expected to scale with organism size. Thus, the size scale of odor patches could range from centimeters to 100 m or more with nektonic organisms. There are, however, volumetric and energetic constraints on increasing body size and, therefore, odorant release mass. Pheromones, for instance, are energetically expensive to produce and store in quantity. In the deep sea most organisms are resource-constrained and small in size (Marshall, 1971). The simulations in Figure 3 illustrate the enormous benefits in terms of size of odor fields that derive from increasing olfactory sensitivity. Threshold sensitivities of several orders of magnitude higher than the goldfish values used here have been reported in vertebrates and in deep-sea fishes highly elaborate olfactory organs have evolved that are indicative of high sensitivity to odor cues (e.g. Marshall, 1967; Baird *et al.*, 1990). We would expect natural selection to favor high olfactory sensitivity in pelagic species where long range detection of chemical signals is important to organism survival.

Olfactory systems evolve so as to maximize the probability of biologically useful outcomes (in the sense of fitness/survival) occurring from the sensing of chemical information in the environment. A given olfactory system will be adapted in its performance characteristics as mediated by the functional needs of the organism, its evolutionary history and the natural environment. These performance parameters include such things as odor specific threshold sensitivities, dynamic response range, scalar sensitivities and appropriate behavioral responses.

A number of authors have discussed in detail the role of

chemical signals in the biology of animals (e.g. Wilson and Bossert, 1963; Hodgson and Mathewson, 1978; Atema, 1988; Sorensen, 1992; Weissburg and Zimmer-Faust, 1993). Most odor cues are substances released by animals (and plants) into the environment that carry biologically significant information to receiving organisms and, when sensed, elicit reactions appropriate to that information. In the ocean, chemoreception brings information that cannot be easily transmitted by other sensory modalities such as vision and/or provides information at greater ranges than is possible with other sensory capabilities. Our concern here is not to explore in depth the sensory physiology, orientation and behavioral responses of aquatic organisms, but rather to examine several of the major ecological consequences of the relationship between hydrodynamics and chemoreception as revealed in our simulations.

Several consequences are immediately apparent. The two most obvious are the basic geometry of dispersion and the rate of dissipation due to 'effective' turbulence. In the mixed layer, the three-dimensional spreading and rapid reduction of odor concentration means that while signals are transmitted rapidly, they are quickly diluted and turbulence rapidly introduces small time/space heterogeneities in signal intensity. The ideal spherical geometry also breaks down both with distance from the source and with time if odor release is periodic. Under these conditions, detection at longer ranges requires high olfactory sensitivity because of the rapid signal attenuation. Where location of the emitting organism may be important, as with a pheromone system, then we would expect such a system to be most effective in the 'near field' if olfaction alone is used for location. The location of an individual female ready to spawn in an aggregation of individuals especially at night when visual perception distances are greatly reduced is one such case.

While there is rapid attenuation of signal strength in the turbulent surface layer, chemoreception may, nonetheless, be important under a number of circumstances, some unrelated to reproduction. Aggregations of organisms release substances either continuously or periodically that provide a considerably larger mass of chemical signal than is possible with a single individual. In such cases, odor patches could be carried quite rapidly and considerably further than the few meters indicated in our simulations. Likewise organisms (or aggregations), whether moving or stationary, may broadcast a chemical signal beyond normal visual perception distances. This is particularly true when visual perception distances are limited due to low light intensities or cryticity of targets. In these cases useful information is potentially available via chemoreception about the presence, numerical abundance and identification of odor causing organisms.

The case where pheromones are released at a depth of 300 m has been explored by Jumper and Baird (1991). Given sufficient olfactory sensitivity pheromone signals can be detected at considerable distances at this depth where ambient light intensities are low. If emitting organisms remain stationary with respect to the center of an active odor patch, the long residence times of pheromone fields and the limited dispersion in the vertical provide excellent conditions for source location.

Since 'effective' turbulence at 300 m still disperses odors fairly rapidly albeit primarily in two dimensions, odor signals could be potentially useful at these depths for non-reproductive purposes as well. Slow moving or stationary organisms could potentially be perceived at ranges close enough in time and space to ensure a high probability of encounter (or avoidance). Likewise large organisms or aggregations of predators or prey that might remain in limited depth horizons could be perceived and identified by olfaction at ranges well in excess of visual perception. Organisms moving relatively rapidly in the vertical may leave little in the way of a useful odor signal.

At 1000 m resident organisms are at the limits of visual perception (Denton, 1990) and chemical signals disperse exceedingly slowly. Where the releasing organism remains stationary for long periods, pheromones could be particularly effective for both long-range detection and source location. There is high coherence in the geometry of the dispersing field and concentration gradients are not rapidly degraded by turbulent motion. If olfactory organs have high sensitivity then our results indicate that impressive perception distances can be achieved. However, chemoreception may be less useful for source location in non-reproductive contexts as odor cues from individual organisms are less likely to carry a signal far enough fast enough to be useful to sparse populations of predators or prey for example. There is some indirect evidence in support of this notion. For instance, Marshall (1967) found that in females of most bathypelagic fishes he studied, olfactory organs were regressed or microsomatic. Likewise, Baird and Jumper (1993) found microsomatic organs in both sexes of the deep living hatchetfish *Sternoptyx diaphana*.

It has been shown that at least in the atmosphere and under advective flow conditions such as in estuaries or streams, turbulence renders odor concentrations in a patch very heterogeneous when measured at fast temporal and small spatial scales exhibited by many individual chemo-

sensory organs (e.g. Murlis and Jones, 1981; Elkinton *et al.*, 1984; Moore, *et al.*, 1994). While additional research is clearly needed to better understand signal heterogeneity in oceanic odor patches we can make several relevant observations based on the few studies cited previously. The time space scales used in obtaining the results in Figure 4 are on the order of 100 cm^3 of volume sampled per min over a space of a meter or so. Studies of individual olfactory organs in marine animals indicate much faster response times and smaller spatial scales. For certain insects, this is on the order of millimeters and centimeters or less (Elkinton *et al.*, 1984). The first antennae of the American lobster is an olfactory organ that samples by flicking through a segment of water at rates as high as 4 Hz (Berg *et al.*, 1992). Nevitt (1991) has provided a basis for olfactory sampling rates in teleost fishes. Over a broad range of fish sizes water exchange in the nasal capsules of flounders occurs in about 250 ms every 2 s with episodes of complete volume replacement every one to two min. Fish then can sample at two temporal scales measured in seconds and minutes utilizing both nasal capsules.

Doving *et al.* (1977) in their studies of the functional anatomy of the olfactory organ in fishes indicate that unlike the pulsed flow in flounder, many species maintain a constant flow across the lamellae of the nasal rosette. Water flows across the lamellar (sensory) surface are aided by ciliary action and are relatively insensitive to swim velocity. This results in a water sample that is well mixed in the anterior nasal chamber before passing across the sensory lamellae over a period of 3–6 s. This slow passage makes imprecise the sensing of the exact timing of microsecond variations in signal strength.

In considering the animal orientation and source location problem at the three depths studied here, we know that dispersion is symmetrical around the release point so that there are no directional cues provided independent of the patch itself (i.e. no substrate or current to be sensed). Under these conditions, the problem collapses to a few variables, namely sensed odor concentration and the time/space scales of change in that concentration as perceived by the receiving organism as it moves in three dimensions. Outside of information inherent in the chemical composition of odor causing substances, these variables are the principal useful cues available for source location.

Whatever the inhomogeneities caused by turbulence, the signal variance will be gaussian in form and can be described as a function of time and distance from the source. The probability of encountering odor concentration peaks of a given concentration due to turbulence decreases rapidly with distance from the source and the relationship of peak strength with distance scales with the initial release mass. Since data are unavailable on small scale odor profiles in the environments modeled here, we can only speculate on their dynamics and therefore the degree to which the model differs from reality in describing the active space sensed by a receiving organism. From studies in highly turbulent environments such as air (Elkinton *et al.*, 1984) or flowing water (Moore *et al.*, 1994) we know that odor profiles are very heterogeneous in small scale space/time which results in odor pulses of threshold or higher concentrations being present at greater ranges from the source than predicted by the model. The higher the degree of turbulence, the greater the likelihood of active patches of odor exceeding the mean values predicted by the model. Nonetheless, as one moves from the source the mean odor pulse decreases rapidly with distance as the model predicts, thereby capturing much of the extant volume of an active odor patch.

To locate a source by olfaction, an organism, once an odor signal is perceived, must sample often and make purposeful movements in response to that perception. Much quantitative information is available early on. An above threshold signal indicates the presence of an emitting source. The average strength of the signal based upon multiple samples in time/space after short-term movement of the organism could carry significant information about the distance to the source. One or a combination of these could elicit the appropriate search behavior by the receiving organism. What is important is the ability of the organism to derive pattern from the integration of the input of many sensory cells over space and time while sampling the environment. In the case of some insects sensing a single threshold signal is sufficient to elicit flight behavior (Elkinton *et al.*, 1984). The initial orientation of the receiving organism can be entirely random as long as it can sense directional movement in swimming. Since odor dispersion is symmetrical around the source in our examples, if on average higher or lower signal strengths are sensed after significant movement then directional information can be gained (Jumper and Baird, 1991). Successfully tracking a gradient depends on both movement and the ability to discriminate differences in odor concentration. Jumper and Baird (1991) in model simulations indicate that numerous changes in direction and backtracking are required even with well-developed discriminatory ability to affect source location.

Weissburg and Zimmer-Faust (1993) observed similar behavior in crabs searching for an odor source in the absence of directional water movement (currents).

For the mixed layer, our models are only gross approximations of the active odor space. This means that there will be a volume beyond that bounded by the threshold concentration over which the probability of encountering a small scale patch of supra threshold concentration falls to zero. The size of this boundary 'layer' is dependent on the degree of turbulence. The difference between model and actual can be expected to be highest near the surface and decrease with depth in the mixed layer. The model is useful in mimicking the general physics of the problem, however, and provides a great deal of understanding about the gross time/space scales of a diffusing odor field.

For instance, the rapid deterioration of patch geometry coupled with marked heterogeneity in signal strength may make exact location by olfaction of the source difficult except in the very near field. Olfactory cues could, however, elicit search behavior in which the probability of perceiving the emitting organisms using both olfaction and other sensory modes (e.g. vision) is greatly enhanced. For example, sharks and tuna are known to have high olfactory sensitivity (Atema *et al.*, 1980) yet generally the actual encounter of prey is by visual perception. The pre-ovulatory pheromone system in goldfish is a case where olfaction provides cues about spawning ready females. The hormone, however, serves only to physiologically stimulate changes in the males, not to mediate mate location.

A number of earlier investigations on chemoreception, primarily from studies of elasmobranchs, were reviewed by Kleerekoper and Gruber (1975), Kleerekoper (1978), and Hodgson and Mathewson (1978). These authors studied chemoreception and orientation to chemical cues in sharks under a variety of experimental and natural conditions. They found that certain natural substances are highly attractive to these fishes in very low concentrations, that when sensed changes in locomotory patterns result and that latency and adaptation to the stimulus are always present. Certain sharks can locate odor sources in the absence of visual cues while in others both visual and olfactory cues are involved in source location. There are marked differences in the ability to detect odor gradients among species, but the strength of the chemical gradient is important to precise odor source location. The presence of flow or current vectors greatly aided source location. In no-flow environments sharks were less likely to precisely locate the exact source of odor emission and required many more turns to reach the immediate vicinity of the source than in flowing waters. These observations are consistent with many of the ideas presented here and provide a basis for future investigations on location and orientation.

At depths of 300 and 1000 m odor patches are much less subject to turbulent eddy diffusivity and little distortion of dye patches were observed at scales of 200 m or less (Ewart and Bendiner, 1981). The very limited vertical extent of a diffusing odor patch results in an abrupt transition in signal strength as one traverses a patch vertically. Under these conditions a searching organism might be expected to perceive an odor field quite similar to that depicted by the model. In the experiments of Schuert (1970), and Ewart and Bendiner (1981) the log scale of concentration gradients of dye release at scales of 200 m or less are on the order of 3–20 m in width with a resolution of $\pm$1–2 m (Figure 4). A small fish moving at about 3.6 cm/s (about a body length/s) would cover 2 m in 1 min. At a sampling rate of once every 2 s (as in flounder) the fish would have taken 30, 250-ms samples into the nasal rosettes over a distance of 2 m. Every 2 min or 4 m a complete evacuation of the rosettes occurs. In lobster, chemoreceptor cells can follow 4-Hz pulses and estimated temporal sampling scales are between 100 and 500 ms (Gomez *et al.*, 1994; Moore *et al.*, 1994). For fishes with constant flow nasal organs (most deep-sea fishes) samples are integrated over a 3–6 s interval. For individual receptors such stimulus patterns as pulse slope, pulse length and off-time are also important in the temporal response of individual cells.

Moore *et al.* (1994) measured odor concentration profiles at fixed distances from a source in turbulent flowing waters in test flumes. Using a 50-ms sampling frequency over a minute they found that with the very heterogeneous signals observed, odor bursts (times when odor was present) were on the order of 5–10 s. Odor concentration peaks (rapid increases in odor concentration) ranged from 0.6 to 2 s. A fish sampling over 250 ms every 2 s over a minute would capture all of the bursts and many of the peaks in a minute's time.

These sampling schemes provide significant time/space resolution of an odor field. If the dynamic range and sensitivity of the receiving olfactory organ is also well developed, then source location can be accomplished at considerable range. The source location problem at 300 m was modeled by Jumper and Baird (1991). Using a mean fish swim speed of 3 cm/s and time/space resolution similar to this model, source locations within a meter were routinely accomplished in simulations assuming very simple search

strategies (albeit with many changes in direction). The critical point is that source location in symmetrically dispersing odor patches presents a different set of problems for the receiving organism than that encountered where there is directional flow (e.g. Kleerekoper and Gruber, 1975). Note that in these simulations organisms and odor fields are subject to the identical bulk movement (i.e. mass flow) of large scale currents and eddies.

These simulations also provide for a greater appreciation of the potential importance of olfactory stimuli to critical ecosystem processes in the sea as a function of depth. Chemical signals have the potential to significantly increase perception distances particularly when other sensory modes have limited range (e.g. vision at depth, at night, with cryptic targets). Since encounter probabilities are exponential functions of the mean distance at which a searching organism perceives (i.e. the perception distance) the object of search, mechanisms which increase perception distance can have profound effects on the encounter dynamics of organisms in the sea. Encounter probabilities are usually calculated as $[1 - \exp(-Zt)]$ where the encounter rate Z is taken to be constant and equal to $[4\pi/3(d_p)^2NV]$ (Gerritsen and Strickler, 1977; Baird and Jumper, 1995). N is a number density and V is a velocity term. The parameter d_p is the mean distance at which a target is perceived. The sensory modes for d_p are unspecified in the general expression, yet the term d_p can depend critically on olfactory sensitivity. Perception distances from odor cues can be considerably larger than for other senses in many environmental circumstances in the ocean as illustrated in Figure 3.

Perception distances because of their non-linear relationship to encounter rates can impact important transfer functions in oceanic ecosystems such as mate location and predator–prey dynamics. Modest increases in olfactory sensitivity are magnified in terms of increasing encounter probabilities by reason of the non-linear relationship with the areal extent of the odor patch (e.g. Figure 3). As shown above the radial extent of the odor patch (d_p) is, in turn, a non-linear function of encounter probability. Baird and Jumper (1995) estimate that for a common mesopelagic fish where both sexes are moving randomly at one body length per second, an increase in perception distance from 0.5 to 2.5 m will reduce the time for a female to encounter a mate at a probability of 0.95 from about 30 days to 1 day. If perception distances can be increased to 5–6 m, the time to encounter can be reduced to about 6 h. The frequency of encounter between predator and prey largely determine energy transfer rates at secondary trophic levels in the open ocean. Odor cues undoubtedly play a significant, but as yet not well understood role in oceanic encounter dynamics.

Olfaction is a unique sensory modality, one that promises to be extremely important in understanding the biology of marine organisms. As shown here, various physical environments can have dramatically different effects in modulating the dynamics of odor dispersal and, therefore, the potential biological utility of chemical stimuli in that environment.

ACKNOWLEDGEMENTS

We would like to thank P.W. Sorenson for providing us with information on goldfish pheromones. We are indebted to G. Patterson, M. O'Neil for text and graphic support, and to J. Atema and his colleagues for valuable insight. This work was partially funded by a grant from Rodney Hunt Company and by a grant from US Advanced Research Projects Agency through the Enterprise Computing Institute.

REFERENCES

Angel, M.V. (1994) Long term, large scale patterns in marine pelagic systems. In: Giller, P.S., Hildrew, A.G. and Raffaelli, D.G. (eds), *Aquatic Ecology: scale, pattern and process*. Blackwell, London, pp. 403–440.

Atema, J. (1988) Distribution of chemical stimuli. In: Atema, J., Fay, R.R., Popper, A.N. and Tavolga, W.N. (eds), *Sensory Biology of Aquatic Animals*. Springer, New York, pp. 13–25.

Atema, J., Holland, K. and Ikehara, W. (1980) Olfactory responses of yellowfin tuna to prey odors: chemical search image. *J. Chem. Ecol.*, **6**, 457–465.

Atema, J., Moore, P.A., Madin, L.P. and Gerhardt, G.A. (1991) Subnose 1: electrochemical tracking of odor plumes at 900 m beneath the ocean surface. *Mar. Ecol. Prog. Ser.*, **74**, 303–306.

Baird, R.C., Jumper, G.Y. and Gallaher, E.E. (1990) Sexual dimorphism and demography in two species of oceanic midwater fishes (Stomiiformes, Sternoptychidae) from the eastern Gulf of Mexico. *Bull. Mar. Sci.*, **47**, 561–566.

Baird, R.C. and Jumper, G.Y. (1993) Olfactory organs in the deep sea hatchetfish *Sternoptyx diaphana* (Stomiiformes, Sternoptychidae). *Bull. Mar. Sci.*, **53**, 1163–1167.

Baird, R.C. and Jumper, G.Y. (1995) Encounter models and deep-sea fishes: numerical simulations and the mate location problem in *Sternoptyx diaphana* (Pisces, Sternoptychidae). *Deep-Sea Res. 1*, **42**, 675–696.

Batchelor, G K. (1950) The application of similarity theory of turbulence to atmospheric diffusion. *Q. J. Roy. Met. Soc.*, **76**, 133–146.

Berg, K., Voight, R. and Atema, J. (1992) Flicking in the lobster *Homarus americanus*: recordings from electrodes implanted in antennular segments. *Biol. Bull.*, **183**, 377–378.

Caldwell, D.R. (1983) Small-scale physics of the ocean. *Rev. Geophys. Space Phys*, **21**, 1192–1205.

Csanady, G.T. (1966) Dispersal of foreign matter by the currents and eddies of the Great Lakes. In *Proceedings of the Ninth Conference on Great Lakes Research*, pp. 283–294.

Csanady, G.T. (1973) *Turbulent Diffusion in the Environment*. D. Reidel Publ. Co., Boston.

Curtis, J.B. and Wood, C.M. (1991) The function of the urinary bladder *in vivo* in the freshwater rainbow trout. *J. Exp. Biol.*, **15**, 567–583.

Denman, K.L. (1994) Scale determining biological-physical interactions in oceanic food webs. In: Giller, P.S., Hildrew, A.G. and Raffaelli, D.G. (eds), *Aquatic Ecology: scale, pattern and process*. Blackwell, London, pp. 377–402.

Denton, E.J. (1990) Light and vision at depths greater than 200 m. In: Herring, P.J., Campbell, A.K., Whitfield, M. and Maddock, L. (eds), *Light and Life in the Sea*. Cambridge University Press, Cambridge, pp. 127–148.

Derby, C.D. and Atema, J. (1988) Chemoreception cells in aquatic invertebrates: peripheral mechanisms in chemical signal processing in decapod crusteceans. In: Atema, J., Fay, R.R., Popper, A.N. and Tavolga, W.N. (eds), *Sensory Biology of Aquatic Animals*. Springer, New York, pp. 366–385.

Doving, K.B., Dubois-Dauphin, M., Holly, A. and Jourdan, F. (1977) Functional anatomy of the olfactory organ of fish and the ciliary mechanism of water transport. *Acta Zool. (Stockholm)*, **58**, 245–255.

Elkinton, J.S., Carde, R.T. and Mason, C.J. (1984) Evaluation of time-average dispersion models for estimating pheromone concentrations in a deciduous forest. *J. Chem. Ecol.*, **10**, 1081–1108.

Ewart, T.E. and Bendiner, W.P. (1981) An observation of the horizontal and vertical diffusion of a passive tracer in the deep ocean. *J. Geophys. Res.*, **86**, 10974–10982.

Finger, T.E. (1988) Organization of chemosensory systems within the brains of bony fishes. In. Atema, J., Fay, R.R., Popper, A.N. and Tavolga, W.N. (eds), *Sensory Biology of Aquatic Animals*. Springer, New York, pp. 118–133.

Gerritsen, J. and Strickler, J.R. (1977) Encounter probabilities and community structure in zooplankton: a mathematical model. *J. Fish Res. Bd. Can.*, **34**, 73–82.

Giller, P S , Hildrew, A.G. and Raffaelli, D.G. (eds) (1994) *Aquatic Ecology: scale, pattern and process*. Blackwell, London.

Gomez, G., Voight, R. and Atema, J. (1994) Frequency filter properties of lobster chemoreceptor cells determined with high resolution measurement. *J. Comp. Physiol.*, **174**, 803–811.

Gregg, M.C. (1987) Diapycnal mixing in the thermocline: a review. *J. Geophys. Res.*, **92**, 5249–5286.

Hara, T.J. (1986) Role of olfaction in fish behavior. In: Pitcher, T.J. (ed.), *Behavior of Teleost Fishes*. Croom Helm, London, pp. 152–176.

Hodgson, E.S. and Mathewson, R.F. (1978) Electrophysiological studies of chemoreception in elasmobranchs. In: Hodgson, E.S. and Mathewson, R.F. (eds), *Sensory Biology of Sharks, Rays and Skates*. US Government Printing Office, Washington, DC, pp. 227–268.

Holland, W.R. and Rhines, P.B. (1980) An example of eddy-induced ocean circulation. *J. Phys. Oceanogr.*, **10**, 1010–1031.

Joseph, J. and Sendner, H. (1958) Über die horizontale Diffusion im Meere. *Dt. Hydrogr. Z.*, **11**, 49–77.

Jumper, G.Y. and Baird, R.C. (1991) Location by olfaction: a model and application to the mating problem in the deep-sea hatchetfish *Argyropelecus hemigymnus*. *Am. Nat.*, **138**, 1431–1458.

Kennish, M.J. (1994) *Practical Handbook of Marine Science*. CRC Press, Boca Raton, Florida.

Kleerekoper, H. (1969) *Olfaction in fishes*. Indiana University Press, Bloomington.

Kleerekoper, H. (1978) Chemoreception and it's interactions with flow and light perception in location and orientation of some elasmobranchs. In: Hodgson, E.S. and Mathewson, R.F. (eds), *Sensory Biology of Sharks, Rays and Skates*. US Government Printing Office, Washington, DC, pp. 269–329.

Kleerekoper, H. and Gruber, D. (1975) Accuracy of localization of a chemical stimulus in flowing and stagnant water by the nurse shark, *Ginglymostoma cirratum*. *J. Comp. Physiology*, **98**, 257–275.

Levin, S.A. (1990) Physical and biological scales and the modeling of predator-prey interactions in large marine ecosystems. In: Sherman, K., Alexander, L.M. and Gold, D.B. (eds), *Large Marine Ecosystems: patterns, processes and yields*. AAAS, Washington, DC, pp. 179–187.

Marshall, N.B. (1967) Olfactory organs of bathypelagic fishes. *Symp. Zool. Soc. Lond.*, **19**, 57–70.

Marshall, N.B. (1971) *Explorations in the Life of Fishes*. Harvard University Press, Cambridge, MA.

Moore, P.A. and Atema, J. (1991) Spatial information in the three-dimensional fine structure of an aquatic odor plume. *Biol. Bull.*, **181**, 408–418.

Moore, P.A., Weissburg, M.J., Parrish, J.M., Zimmer-Faust, R.K. and Gerhardt, G.A. (1994) Spatial distribution of odors in simulated benthic boundary layer flows. *J. Chem. Ecol.*, **20**, 255–279.

Moulton, D.G. and Marshall, D.A. (1976) The performance of dogs in detecting x ionone. *J. Comp. Phys.*, **110**, 287–306.

Murlis, J. and Jones C.D. (1981) Fine scale structure of odor plumes in relation to insect orientation to distant pheromone and other attractant sources. *Physiol. Entomol.*, **6**, 71–86.

Murthy, C.R. (1976) Horizontal diffusion characteristics in Lake Ontario. *J. Phys. Oceanogr.*, **6**, 76–84.

Nevitt, G.A. (1991) Do fish sniff: a new mechanism of olfactory sampling in pleuronectid flounders. *J. Exp. Biol.*, **1501**, 1–18.

Okubo, A. (1971) Oceanic diffusion diagrams. *Deep-Sea Res.*, **18**, 789–802.

Okubo, A. (1980) *Diffusion and Ecological Problems: mathematical models*, Biomathematics, Vol. 10. Springer, New York.

Parslow, J.S. and Gabric, A.J. (1989) Advection, dispersal and plankton patchiness on the Great Barrier reef. *Aust. J. Mar. Freshwater Res.*, **40**, 403–419.

Pickart, R.S. (1988) Entrainment and homogenization of a passive tracer in a numerical model gyre. *J. Geophys. Res.*, **93**, 6761–6773.

Rittschoff, D. (1992) Chemosensation in the daily life of crabs. *Am. Zool.*, **32**, 363–369.

Ross, D.A. (1988) *Introduction to Oceanography*. Prentice Hall, Englewood.

Roughgarden, J., Gaines, S. and Possingham, H. (1988) Recruitment dynamics in complex life cycles. *Science*, **241**, 1460–1466.

Schuert, E.A. (1970) Turbulent diffusion in the intermediate waters of the N. Pacific Ocean. *J. Geophys. Res.*, **75**, 673–682.

Sorensen, P.W. (1992) Hormones, pheromones and chemoreception. In: Hara, T.J. (ed.), *Fish Chemoreception*. Chapman and Hall, London, pp. 199–228.

Sorensen, P.W. and Stacey, N.E. (1990) Identified hormonal pheromones in the goldfish: the basis for a model of sex pheromone function in teleost fish. In: MacDonald, D.W., Muller-Schwarze, D. and Matynczuk, S.E. (eds), *Chemical Signals in Vertebrates V.* Oxford University Press, Oxford, pp. 302–314.

Weissburg, M.J. and Zimmer-Faust, R.K. (1993) Life and death in moving fluids: hydrodynamic effects on chemosensory-mediated predation. *Ecology*, **74**, 1428–1443.

Westerberg, H. (1991) Properties of aquatic odor trails. In: Doving, K. (ed.), *Proceedings of the Tenth International Symposium on Olfaction and Taste*. Graphic Communication System, Oslo, pp. 45–65.

Wilson, E.O. and Bossert, W.K. (1963) Chemical communication among animals. *Recent Prog. Horm. Res.*, **19**, 673–716.

Received on January 9, 1995; accepted on December 6, 1995